Rapid In-Situ Carbon and Oxygen Cleaning of $In_{0.53}Ga_{0.47}As(001)$ and $Si_{0.5}Ge_{0.5}(110)$ Surfaces via a H_2 RF Downstream Plasma

S. Wolf[a], M. Edmonds[a], X. Jiang[b], R. Droopad[c], N. Yoshida[d], L. Dong[d], R. Galatage[e], S. Siddiqui[e], B. Sahu[e] and A. Kummel[f]

[a] Materials Science and Engineering Program, University of California San Diego, La Jolla, California 92093, USA
[b] PIE Scientific LLC, San Mateo, California 94402, USA
[c] Ingram School of Engineering, Texas State University, 601 University Dr, San Marcos, Texas 78666, USA
[d] Applied Materials Inc, 974 E Arques Ave, Sunnyvale, California 94085, USA
[e] GLOBALFOUNDRIES, 400 Stone Break Rd Extension, Malta, New York 12020, USA
[f] Department of Chemistry, University of California San Diego, La Jolla, California 92093, USA

The $In_{0.53}Ga_{0.47}As(001)$ and $Si_{0.5}Ge_{0.5}(110)$ surfaces were cleaned using a downstream RF plasma. On the air-exposed $In_{0.53}Ga_{0.47}As(001)$ surface, a 2 second 100 millitorr H_2 plasma dose fully removed carbon and oxygen. On the ex-situ wet cleaned $Si_{0.5}Ge_{0.5}(110)$ surface, nearly all carbon and oxygen are removed via a 2 second exposure of 5% H_2 in Ar plasma. To prevent oxygen deposition from the plasma tube while maximizing the atomic H flux, for $Si_{0.5}Ge_{0.5}(110)$, the plasma power, pressure, and gas composition must be controlled. The $Si_{0.5}Ge_{0.5}(110)$ surface is more sensitive than the $In_{0.53}Ga_{0.47}As(001)$ surface to trace oxygen in the plasma stream consistent with the higher heat of formation per Si of SiO_2 than the heat of formation per Ga of Ga_2O_3. The higher heat of formation of SiO_2 is expected to both increase oxygen adsorption and prevent the atomic H from forming volatile products with SiO_2 on $Si_{0.5}Ge_{0.5}(110)$, in contrast to $In_{0.53}Ga_{0.47}As(001)$.

Introduction

As the search continues for new materials to replace silicon in MOS devices, InGaAs and SiGe have demonstrated good potential due to their intrinsically high mobilities. In order to implement these compound semiconductors into devices, the surfaces of these materials must be atomically flat and void of surface defects. To achieve this clean surface, there are various surface cleaning techniques available, including the RCA standard cleaning procedure consisting of various treatments with NH_4OH, H_2O_2, HF, HCl, and H_2O to remove the native oxide and organic and ionic contaminants, UV/ozone treatments, and cleaning via thermal gas crackers and plasma sources (1-5). However, the wet processes can leave organic residues and a thin layer of native oxide on the surface due to exposure to ambient conditions, while the vacuum/dry processing steps can take over 30 minutes to perform. One technique, which overcomes this issue, involves the use of an in-situ plasma source to remove carbon and oxygen present on the surface (6).

When a surface comes in contact with a plasma gas, several interactions can result including sputtering caused by energetic ions, chemical etching with reactive radicals generated in the plasma, and even desorption from the heating of the surface due to bombardment by particles (7). When atomic hydrogen is used to clean the surface, the three common methods of generating neutral atomic H involve downstream plasmas, remote plasmas, and thermal crackers. Compared to downstream plasmas, thermal crackers typically operate at a lower pressure, and therefore, produce a lower atomic H flux. There is also a risk of metal contamination from hot tungsten filaments used in thermal gas crackers (3). Compared to downstream plasmas, remote plasmas have line of sight to the sample, and therefore risk radiation damage to the sample (8). By incorporating the in-situ downstream plasma source and optimized experimental conditions, the efficacy of ion-less plasma treatment for the rapid cleaning of the $In_{0.53}Ga_{0.47}As(001)$ and $Si_{0.5}Ge_{0.5}(110)$ surfaces has been demonstrated.

In this study, X-ray photoelectron spectroscopy (XPS) was employed to characterize the chemical composition of the $In_{0.53}Ga_{0.47}As(001)$ and $Si_{0.5}Ge_{0.5}(110)$ surfaces before and after plasma exposures. To optimize the conditions for cleaning with a plasma source, the effect of plasma power and pressure on carbon cleaning and oxygen contamination were determined. In addition, the effect of pure H_2 versus an H_2/Ar mixture was investigated in relation to the removal of carbon and oxygen contaminants. Using the described approach, carbon and oxygen was removed within two seconds from the $In_{0.53}Ga_{0.47}As(001)$ surface, and nearly all carbon and some oxygen were removed on the $Si_{0.5}Ge_{0.5}(110)$ surface.

Experimental Setup

Sample Preparation

For the $In_{0.53}Ga_{0.47}As(001)$ samples, a 200 nm layer of $In_{0.53}Ga_{0.47}As$ doped with a silicon concentration of $2x10^{18}$ cm^{-3} was grown by molecular beam epitaxy (MBE) on a 500 μm thick commercial grade InP substrate. To protect the surface from contamination and degradation, a 50 nm thick As_2 cap was deposited on the MBE samples and subsequently shipped and stored under vacuum. Once the samples were loaded into the Omicron UHV VT-STM chamber with base pressure less than $1x10^{-10}$ torr, they were degassed at 180°C for 30 minutes, decapped at 330-360 °C for 1 hour, and annealed to 380 °C in order to achieve the pure InGaAs(001)-(2x4) surface reconstruction. The (2x4) surface reconstruction was confirmed through low energy electron diffraction (LEED) measurements and STM images of the surface in a previous study (9).

For the $Si_{0.5}Ge_{0.5}(110)$ samples, a 50 nm thick layer of SiGe was grown on an Si(110) substrate. Prior to being loaded into the vacuum chamber, $Si_{0.5}Ge_{0.5}(110)$ samples underwent a degrease cleaning procedure and wet chemical etch, which consisted of a 10 minute sonication in acetone, a 10 minute sonication in isopropyl alcohol, a 5 minute sonication in HPLC water, followed by a dip into 2% HF/H_2O. To minimize air exposure, the sample was pulled from the HF solution through a protective layer of toluene and placed into a beaker of toluene (5). The sample was then loaded into the vacuum system as quick as possible with an exposure to air of less than one minute to prevent reformation of the surface native oxide layer.

Vacuum System Setup Including Downstream Plasma Source

Samples were introduced into high vacuum at the loading chamber, which was separated from the ALD chamber via a gate valve. Another gate valve separated the loading chamber from the preparation chamber. The preparation chamber had a base pressure of $1x10^{-10}$ torr and contained a monochromatic XM 1000 MkII/Sphera XPS system (Omicron Nanotechnology) for collecting spectra data. A constant analyzer pass energy of 50 eV was employed with a 0.1 eV linewidth obtained using a monochromatic Al Kα source with energy 1486.7 eV. The takeoff angle was 30° relative to the surface with an acceptance angle of 7°. The spectra were then analyzed with CASA XPS v 2.3. The ALD chamber was equipped with a PIE Scientific SEMI-KLEEN plasma cleaner; this chamber had a base pressure of $5x10^{-7}$ torr after baking out the system including all stainless steel tubing at ~100°C for 12 hours. The downstream RF plasma cleaner was equipped with a pressure and temperature sensor, as well as a chemically robust sapphire tube. Figure 1 shows the plasma cleaner that was used in all experiments.

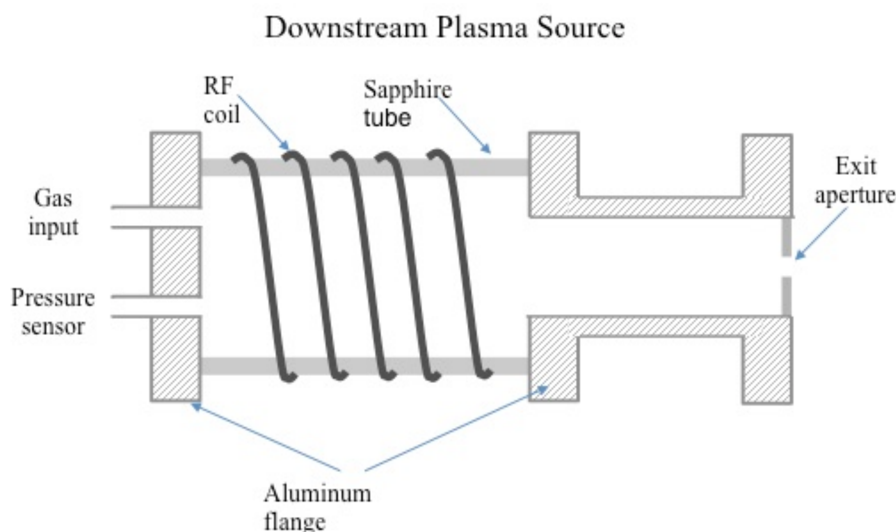

Figure 1. Diagram showing the downstream RF plasma source.

Results

Part 1: $In_{0.53}Ga_{0.47}As(001)$-(2x4) Surface Clean

To test the efficacy of the downstream plasma source with a sapphire tube, the decapped n-type $In_{0.53}Ga_{0.47}As(001)$-(2x4) substrate underwent a series of exposures, as shown in Figure 2. All raw XPS spectra were only normalized to the background intensity. The XPS areas were calculated and plotted first as corrected peak areas by dividing the raw peak area by the Schofield photoionization cross sectional relative sensitivity factors. The corrected peak areas were then normalized to the sum of the contributions from the elemental (i.e. not including higher binding energy components) As 2p 1/2 and 3/2, Ga 2p 1/2 and 3/2, and In 3d 3/2 and 5/2 spin orbit splits. Normalized peak areas were plotted for As 2p, AsO_x, Ga 2p, GaO_x, In 3d, O 1s, and C 1s signals relative to the sum of As 2p + Ga 2p + In 3d. Extensive analysis on the In 3d higher binding energy components was not performed because the contribution was small. For

this paper, Equation 1 was used to calculate the plasma exposures in Langmuirs (L), which assumed 100% dissociation of the H_2; therefore, this was an upper limit approximation for the exposure because the exact H_2 dissociation was not known.

$$\text{Exposure (L)} = 10^6 \text{ x Pressure (Torr) x Time (s)} \quad [1]$$

The clean, decapped surface was dosed with a 2 second, 100 millitorr plasma at 30 W RF power and a surface temperature of 285°C. After the 200,000 L exposure, the As 2p signal was slightly attenuated. It has been reported that atomic arsenic can be converted to a volatile AsH_3 desorption product upon exposure to hydrogen (3, 10). After the first exposure, the sample was exposed to air for 1 hour and was re-introduced into the UHV system. Following the 1 hour air exposure, the oxygen 1s and carbon 1s peaks were present as well as noticeable oxidized components on both the As 2p and Ga 2p spin orbit split signals. On the As 2p 3/2 spin orbit split peak, the oxidized component was at an approximate binding energy of 1326.5 eV, while on the Ga 2p 3/2 spin orbit split peak, the oxidized component was at an approximate binding energy of 118 eV. In the literature, stoichiometric As and Ga oxides have been reported as high as 1327.3 eV and 119 eV, respectively, so it was proposed that these oxides were sub-stoichiometric, AsO_x and GaO_x (11,12).

After air exposure, another 200,000 L 30 W H plasma clean at a substrate temperature of 250°C was performed, which was able to fully remove the carbon and oxygen on the surface. Similarly to the mechanism of forming AsH_3 on the surface, it has also been reported that Ga_2O_3 and As_2O_3 can be reduced to more volatile products by forming an H_2O reaction product when atomic H reacts on the surface (3, 13-15). It was expected that removal of these volatile byproducts would be even easier due to having sub-stoichiometric oxides on the surface. A more in-depth discussion on the thermodynamic treatment of the surface species and how it can explain the atomic H cleaning results will be presented in the discussion and conclusion.

Following this post air exposure H_2 plasma clean, the In, Ga, and As normalized peak areas remained relatively unchanged compared to the clean, decapped $In_{0.53}Ga_{0.47}As(001)$ surface; this demonstrated that this downstream plasma cleaning process can remove unwanted contaminants from the $In_{0.53}Ga_{0.47}As(001)$ surface without causing excessive, unwanted substrate etching and degradation.

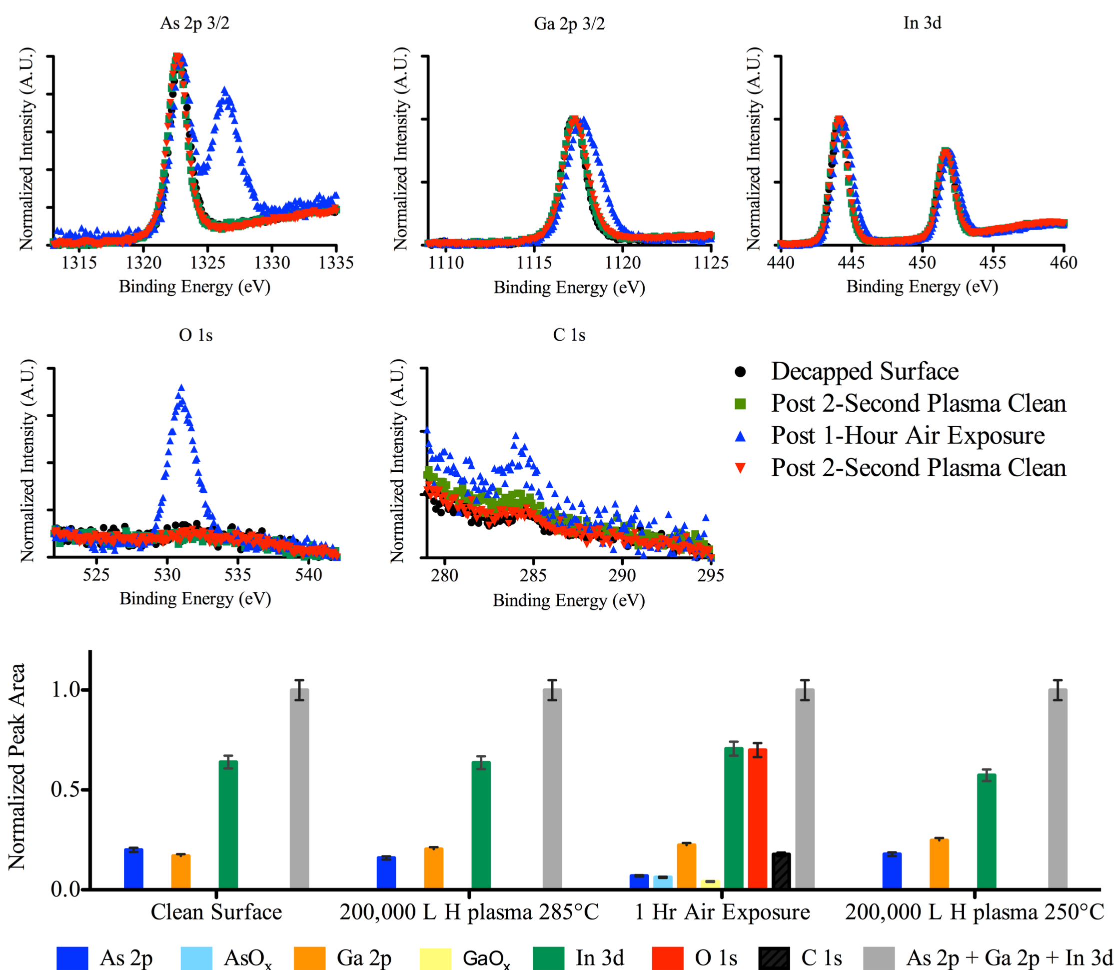

Figure 2. H_2 downstream plasma clean with sapphire tube on $In_{0.53}Ga_{0.47}As(001)$. At the top, XPS raw signals for As 2p 3/2, Ga 2p 3/2, In 3d, O 1s, and C 1s normalized to the background intensity, and at the bottom, XPS corrected peak areas normalized to elemental As 2p + Ga 2p + In 3d for As 2p, AsO_x, Ga 2p, GaO_x, In 3d, O 1s, and C 1s. XPS was collected on the clean InGaAs(001)-(2x4) surface, post-2 second H_2 100 millitorr plasma clean at 285°C, post 1 hour air exposure, and after a final 2 second H_2 100 millitorr plasma clean at 250°C. The plasma clean fully removed carbon and oxygen deposited on the surface with minimal substrate etching.

Part 2: $Si_{0.5}Ge_{0.5}(110)$ Surface Clean

The plasma cleaner with a sapphire tube was tested on the $Si_{0.5}Ge_{0.5}(110)$ surface. However, in the literature, it is well known that the SiGe surface is a difficult surface to clean because wet clean treatments leave the surface unstable in ambient air due to the strong silicon-oxygen bonds formed (16-18). As described in the experimental setup, all $Si_{0.5}Ge_{0.5}(110)$ samples underwent a wet clean procedure prior to being loaded into the UHV chamber.

Since a 2 second, 30 Watt H_2 plasma clean at 100 millitorr completely stripped the oxidized $In_{0.53}Ga_{0.47}As(001)$ surface of carbon and oxygen, the same conditions were

tested on the $Si_{0.5}Ge_{0.5}$(110) surface. Raw XPS spectra for Ge 3d, Si 2p, O 1s, and C 1s normalized to background intensity were plotted at the top of Figure 3. XPS peak areas for Ge 3d, Si 2p, SiO_x, O 1s, and C 1s were corrected and normalized to the sum of elemental Ge 3d and Si 2p for the wet cleaned surface and a 2 second H_2 100 millitorr plasma clean. These processing conditions were only able to reduce the carbon by approximately 66%, so additional plasma exposure times were employed: an extra 10 seconds and an extra 200 seconds of H_2 plasma. When the plasma exposure time increased to several minutes, a small decrease in carbon was seen at the expense of increasing the amount of oxygen on the surface. This effect was most clearly illustrated by the growth of an SiO_x component on the Si 2p peak around binding energy 102.3 eV.

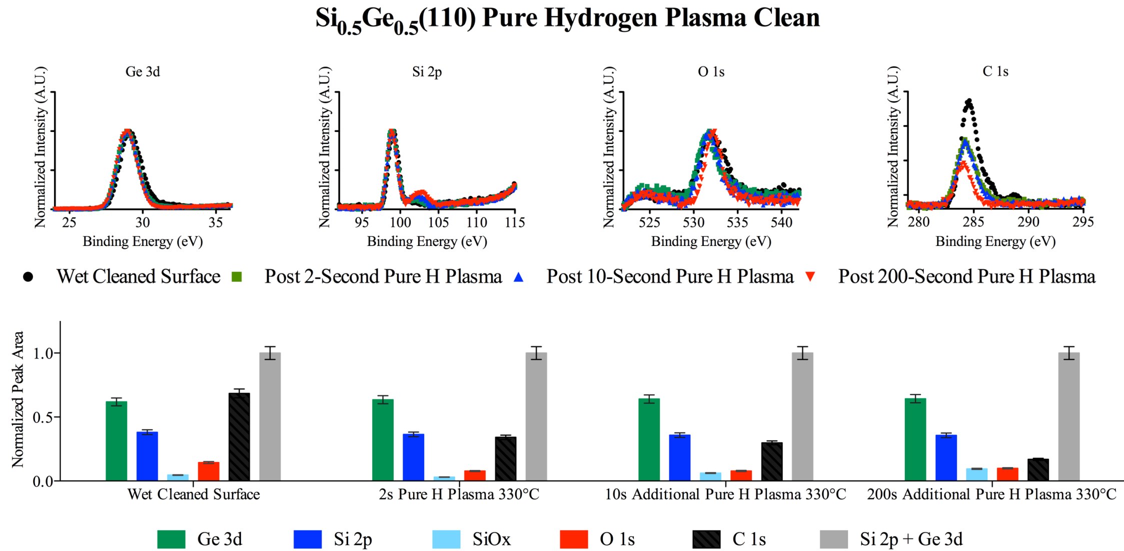

Figure 3. H_2 downstream plasma clean with sapphire tube on $Si_{0.5}Ge_{0.5}$(110). At the top, XPS raw signals normalized to background intensity, and at the bottom, XPS corrected peak areas normalized to elemental Si 2p + Ge 3d for Ge 3d, Si 2p, SiO_x, O 1s, and C 1s on the wet cleaned $Si_{0.5}Ge_{0.5}$(110) surface. The C 1s signal decreased upon subsequent exposures to H_2 plasma, but growth of the higher binding energy Si 2p peak (consistent with SiO_x) occurred for longer exposures times.

It was hypothesized that the oxygen increase could be due to one or a combination of the following problems: chemical etching of the sapphire tube or native oxide on the downstream aluminum chamber/flange due to atomic H, the background O_2/H_2O from the base pressure of the plasma source, or any trace oxygen contained in the source gas. Previous studies have shown that H_2 plasmas can sputter quartz causing the oxygen seen on the surface to increase (19-21). To test if chemical etching from the pure H_2 was causing the increase in oxidized silicon, pure H_2 was switched for a mixture of 5% H_2 in Ar since this was expected to reduce the density of energetic H atoms colliding with the plasma tube; however, this introduced the possibility of physical sputtering of the sapphire tube or aluminum chamber/flange by Ar ions, as the sputtering capability of Ar ions has been well documented in literature (22- 24).

H_2/Ar Plasma Power Optimization on $Si_{0.5}Ge_{0.5}$(110). In order to study the effect of the plasma power with the 5% H_2 in Ar, the plasma power was varied between 30 W and 100 W at a constant substrate temperature of 330°C, a pressure of 100 millitorr, and an exposure of 2 seconds (see Figure 4). From this data, it was seen that both the 30 W and

100 W cleans reduced the carbon below 5% and to 0%, respectively. However, the oxygen peak area increased by 40% after exposure at 100 W. This data was consistent with the Ar ions being sufficiently energetic at 100 W to sputter oxygen from the sapphire tube or aluminum chamber/flange onto the sample. It was expected that at the lower plasma power of 30 W, the amount of sputter by the argon would be reduced. Ultimately, because much less oxygen was deposited, the 30 W clean was deemed a better condition to study the effect of plasma pressure due to the strong carbon removal and minimal oxygen deposition.

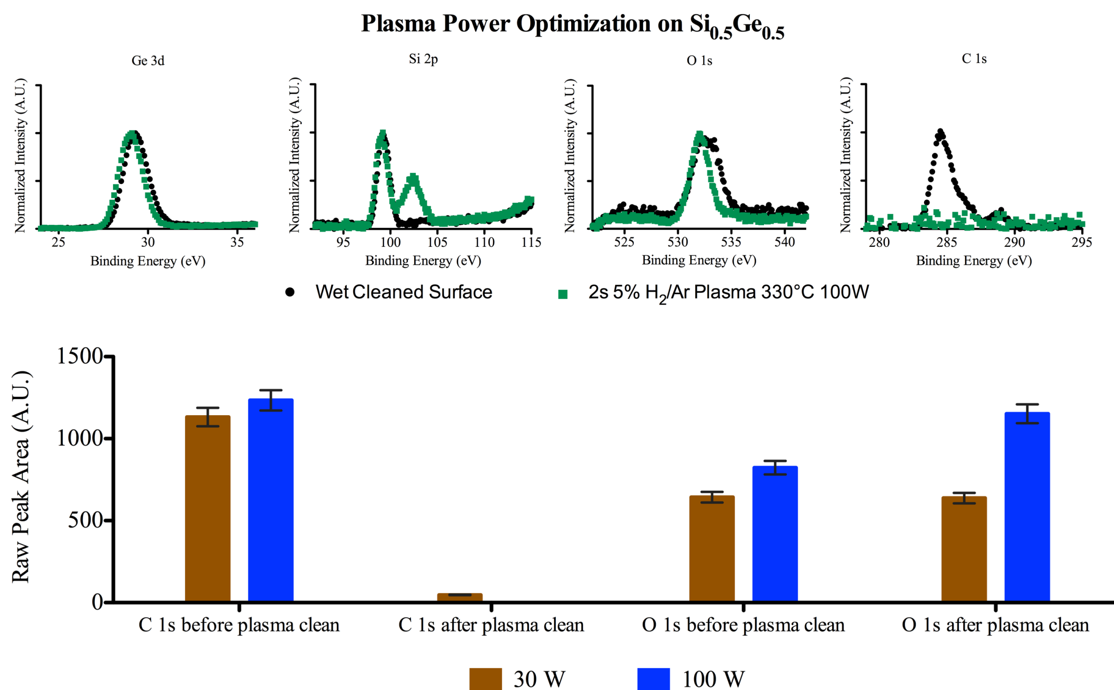

Figure 4. 30 W and 100 W 5% H_2 in Ar downstream plasma clean with sapphire tube on $Si_{0.5}Ge_{0.5}$(110). At the top, XPS raw signals normalized to background intensity for 100 W clean. Note raw XPS spectra for 30 W were plotted in Figure 6. At the bottom, XPS raw peak areas for C 1s and O 1s before and after the 2-second plasma cleans at 30 W and 100 W RF power. The 30 W clean resulted in a significant reduction of the C 1s signal, while not depositing any additional oxygen.

H_2/Ar Plasma Pressure Optimization on $Si_{0.5}Ge_{0.5}$(110). After optimizing the plasma power, a 1 minute plasma clean with 5% H_2 in Ar at a plasma power of 30 Watts was tested at three conditions: (a) a chamber pressure of 18 millitorr and temperature of 100°C (b) a chamber pressure of 100 millitorr and temperature of 330°C and (c) a chamber pressure of 600 millitorr and temperature of 330°C. The Ge 3d, Si 2p, O 1s, and C 1s XPS signals normalized to the background were plotted in the upper portion of Figure 5, along with the corrected C 1s and O 1s areas before and after plasma exposure. For each test, the wet cleaned sample had a large amount of carbon present on the surface, as well as a native oxide from exposure to ambient air upon loading into UHV. At 18 millitorr and 100°C, the 1 minute plasma clean removed nearly 90% of the carbon on the surface, but the oxygen nearly increased by 75%. At 100 millitorr and a temperature of 330°C, the C 1s signal was reduced to noise and the oxygen signal increased 20 to 25%. At 600 millitorr and 330°C, the clean only removed 70% of the carbon, and increased oxygen by almost 80%. It must be noted that the starting amount of carbon and oxygen on the surface varied from sample to sample, depending on the length of air exposure

when loaded into the UHV chamber. Also, the amount of SiO_x was similar in each case, possibly indicating that oxygen in the 100 millitorr experiment that was not bonded to Si before exposure, transferred its bonds to silicon after exposure.

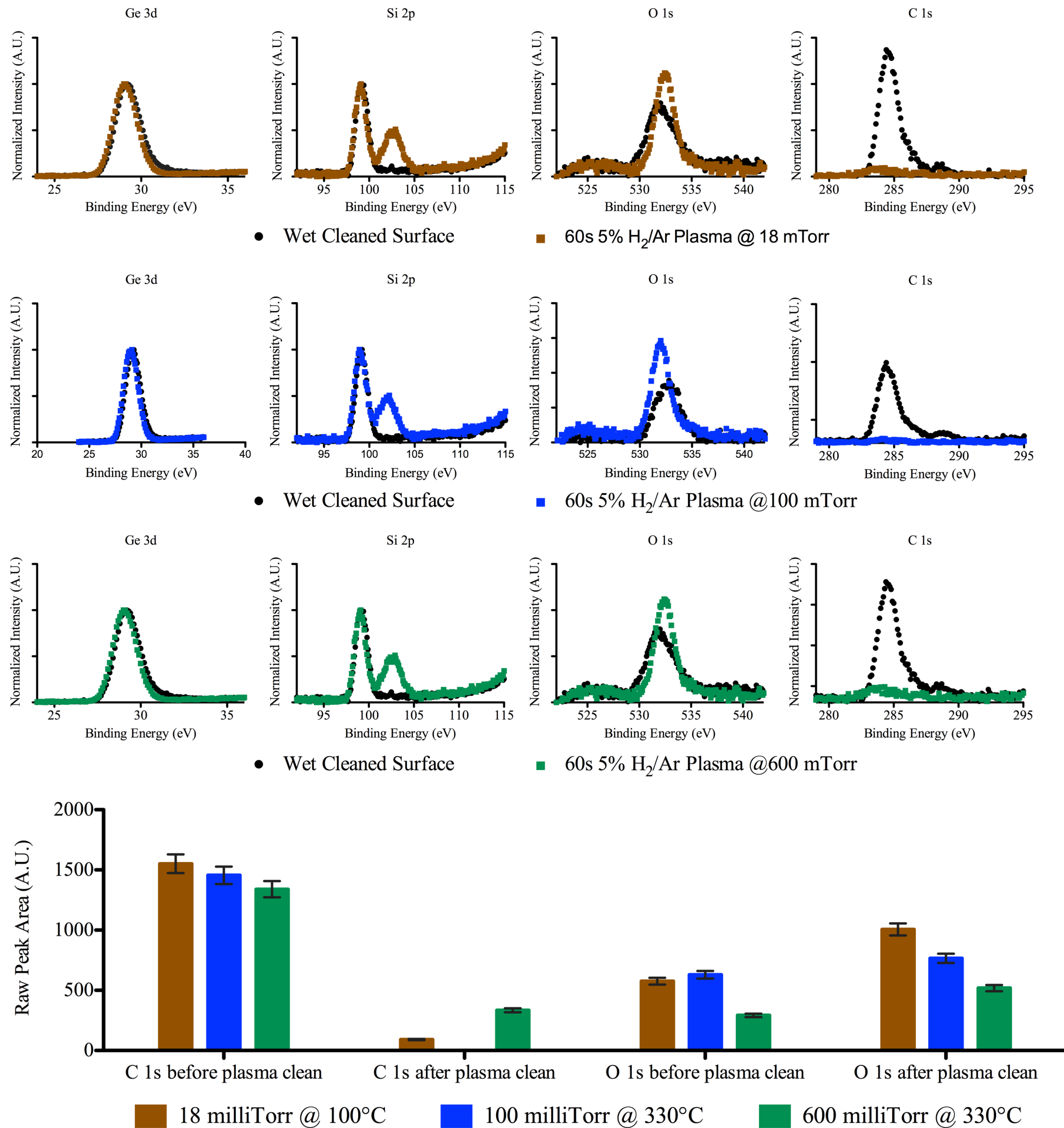

Figure 5. 5% H_2 in Ar downstream plasma clean with sapphire tube on $Si_{0.5}Ge_{0.5}$(110) at 18 millitorr, 100°C; 100 millitorr, 330°C; and 600 millitorr, 330°C. At the top, XPS raw signals normalized to background intensity, and at the bottom, XPS raw peak areas plotted for C 1s and O 1s before and after the 2 second plasma exposures.

At higher pressure, 600 millitorr, it was possible that there was increased hydrogen recombination, which lowered the amount of atomic H reaching the surface, thus impeding the removal of carbon. In addition, since the chamber was evacuated by a turbo pump, for higher pressures, the pumping speed was reduced, thereby increasing the residence time of the gas in the chamber, as well as both gas phase and wall recombination of atomic H. For the 18 millitorr, 100°C experiment, it was hypothesized that a lower temperature and pressure could mean that less oxygen could get on the

sample mainly due to the overall lower dose given to the sample. However, this resulted in far more oxygen getting on the sample than desired, possibly indicating that at lower pressure, the argon ions were more energetic when hitting the plasma tube or aluminum flange/chamber; thereby, increasing the oxygen in the plasma gas.

H_2/Ar Optimized Recipe on $Si_{0.5}Ge_{0.5}$(110). After studying the effects of plasma power and pressure on $Si_{0.5}Ge_{0.5}$(110), an optimized recipe was performed. Figure 6 shows the XPS spectra for the best downstream plasma clean recipe on $Si_{0.5}Ge_{0.5}$(110). A substrate temperature of 330°C, a plasma power of 30 W, 5% H_2 in Ar, and a pressure of 100 millitorr were the conditions used for a 2 second exposure. Note the almost complete removal of the C 1s signal and the narrowing of the O 1s peak that yields an overall slight decrease in the normalized corrected O 1s peak area. A small higher binding energy SiO_x peak at binding energy 102.5 eV formed, indicating oxygen formed bonds to silicon.

Optimized $Si_{0.5}Ge_{0.5}$ (110) H_2/Ar Plasma Clean

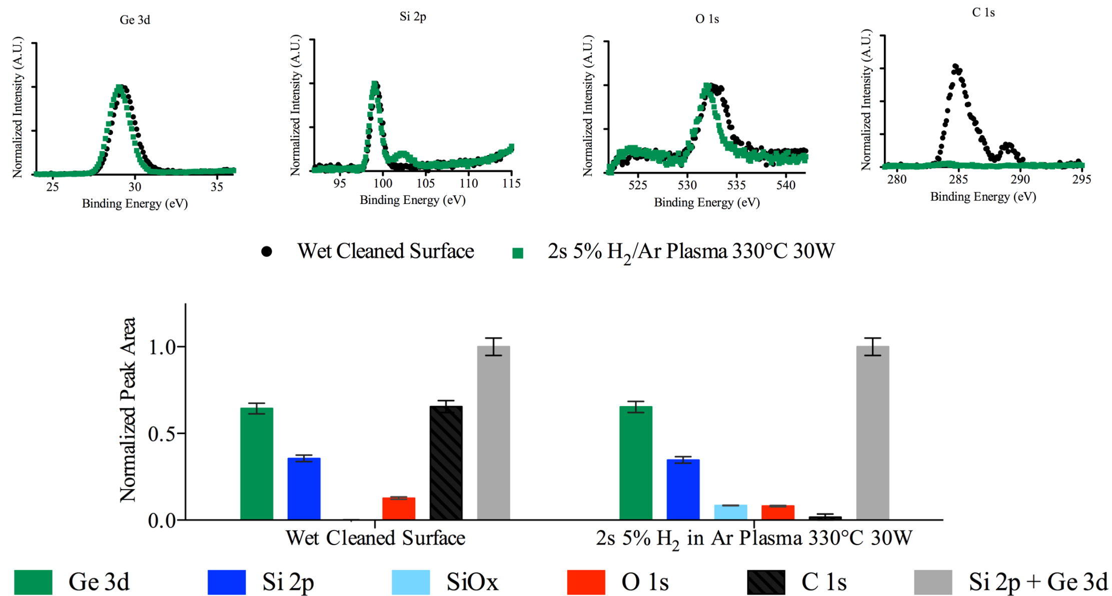

Figure 6. Optimized 5% H_2 in Ar downstream plasma clean with sapphire tube on $Si_{0.5}Ge_{0.5}$(110). A substrate temperature of 330°C, a plasma power of 30 W, and a pressure of 100 millitorr were the parameters used for a plasma dose of 2 seconds. At the top, XPS raw signals normalized to background intensity, and at the bottom, XPS corrected peak areas normalized to elemental Si 2p + Ge 3d for Ge 3d, Si 2p, SiO_x, O 1s, and C 1s.

Discussion and Conclusion

Rapid 2 second cleaning of carbon and oxygen on an air-exposed $In_{0.53}Ga_{0.47}As$(001) surface was achieved by dosing 200,000 L of H_2 plasma at 250°C as verified by XPS measurements. The likely removal of volatile GaO_x and AsO_x species from the surface accounted for the rapid $In_{0.53}Ga_{0.47}As$(001) surface clean. In addition, the downstream plasma did not deposit any additional oxygen on the clean, decapped surface, while minimally etching the substrate.

On the contrary, the $Si_{0.5}Ge_{0.5}(110)$ was not cleaned in such a simple manner; pure H_2 plasma proved ineffective at rapidly removing the carbon and oxygen from the surface. Ultimately, a 2 second, 30 Watts RF power, 100 millitorr 5% H_2 in Ar exposure at 330°C nearly fully cleaned the surface without significantly increasing the amount of oxygen on the surface. It was hypothesized that the $Si_{0.5}Ge_{0.5}(110)$ surface was more efficiently cleaned with the H_2/Ar gas mixture compared to pure H_2 because the Ar was more readily ionized. Since the Ar ionized more readily, the H_2/Ar plasma should have a much higher plasma density (electron/ion density) than the pure H_2 plasma, thereby facilitating the dissociation of H_2 into atomic H. In addition, by employing Ar as a carrier gas, the partial pressure of hydrogen was lower which helped prevent recombination of atomic H. Therefore, it was likely that the flux of atomic H to the surface was higher with the Ar carrier gas.

The oxygen deposition and carbon removal on the $Si_{0.5}Ge_{0.5}(110)$ surface can be explained by looking at the thermodynamics of the species present on the surface. The high heats of formation for solid SiO_2 (-911 kJ/mol) is consistent with the inability to completely strip the oxygen from the surface. Once these bonds are formed, they are quite hard to break. In effect, the high heat of formation for SiO_2 poses two challenges for cleaning of the surface: (1) trace O_2 or H_2O in the plasma gas are likely to form more Si-O bonds and (2) breaking Si-O bonds by atomic H will be unlikely. Note, consistent with the importance of the role of the heats of formation, the heat of formation of SiO_2 is 1.57x the heat of formation of GeO_2 (-580 kJ/mol), so GeO_2 is not observed.

In comparison, the heat of formations of Ga_2O_3 per Ga atom and As_2O_5 per As atom are both smaller than for SiO_2 at only -545 kJ/mol and -463 kJ/mol, respectively. Further, when considering the heat of formation for other oxide species, such as Ga_2O and As_2O_4, the heats of formation decrease further. For carbon bonds to the surfaces, the standard heat of formation for Si-C is only -66 kJ/mol (25). Enthalpies of formation for Ga-C, As-C, and In-C bonds are not readily found in the literature, possibly indicating these bonds are not very stable. Equations [2]-[10] show enthalpy of reaction calculations for various surface species and expected reactions assuming a standard reference state of 0 for atomic H.

$$SiO_2\ (s) + 4H \Rightarrow Si\ (s) + 2H_2O\ (g) \qquad \Delta H = 429\ \text{kJ/mol Si} \qquad [2]$$

$$GeO_2\ (s) + 4H \Rightarrow Ge\ (s) + 2H_2O\ (g) \qquad \Delta H = 100\ \text{kJ/mol Ge} \qquad [3]$$

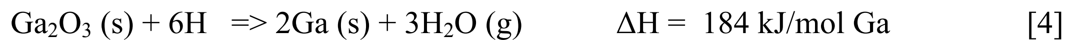

$$Ga_2O_3\ (s) + 6H \Rightarrow 2Ga\ (s) + 3H_2O\ (g) \qquad \Delta H = 184\ \text{kJ/mol Ga} \qquad [4]$$

$$Ga_2O\ (s) + 2H \Rightarrow 2Ga\ (s) + H_2O\ (g) \qquad \Delta H = 58\ \text{kJ/mol Ga} \qquad [5]$$

$$As_2O_5\ (s) + 10H \Rightarrow 2As\ (s) + 5H_2O\ (g) \qquad \Delta H = -280\ \text{kJ/mol As} \qquad [6]$$

$$As_2O_4\ (s) + 8H \Rightarrow 2As\ (s) + 4H_2O\ (g) \qquad \Delta H = -170\ \text{kJ/mol As} \qquad [7]$$

$$In_2O_3\ (s) + 6H \Rightarrow 2In\ (s) + 3H_2O\ (g) \qquad \Delta H = 102\ \text{kJ/mol In} \qquad [8]$$

$$SiC\ (s) + 4H \Rightarrow Si\ (s) + CH_4\ (g) \qquad \Delta H = -9\ \text{kJ/mol Si} \qquad [9]$$

$$GeC\ (g) + 4H \Rightarrow Ge\ (s) + CH_4\ (g) \qquad \Delta H = -707\ \text{kJ/mol Ge} \qquad [10]$$

The heats of formation in equations [2] and [3] for SiO_2 and GeO_2 are highly endothermic, while the Si-C heat of formation in equation [9] is much closer to thermo-neutral, providing a mechanism consistent with the removal of carbon being easier than

the removal of oxygen from SiGe. For the Ga, As, and In oxides (equation [4]-[8]), the reaction enthalpies of formation are much less endothermic, or even exothermic, which is consistent with the ability of atomic H to easily clean InGaAs. In order to achieve a better removal of the oxide on the SiGe surface, it would be necessary to incorporate in-situ fluorine chemistry into the plasma gas mixture or a cyclic clean with H and a common SiO_2 cleaning method, such as NF_3/H_2 or NF_3/NH_3 plasmas. It has been shown in the literature that NF_3 and NH_3 incorporated into H_2 plasma can gently remove native oxide on silicon (26-27).

Acknowledgments

The authors would like to thank Ximan Jiang of Pie Scientific LLC for the use of the PIE Scientific SEMI-KLEEN Remote Plasma Cleaner, as well as GLOBALFOUNDRIES and Dr. Ravi Droopad for supplying the $Si_{0.5}Ge_{0.5}$(110) wafer and $In_{0.53}Ga_{0.47}As$(001) wafer, respectively. Lastly, the authors would like to thank Rasirc for the anhydrous hydrazine. This work was supported by the Semiconductor Research Corporation (Task 2451.001), NSF DMR 1207213, and Applied Materials.

References

1. A. Ishizaka and Y. Shiraki. *J. Electrochem. Soc.* **133**, 666-671 (1986).
2. W. Kern. *J. Electrochem. Soc.* **137**, 1887-1892 (1990).
3. W. Melitz, J. Shen, T. Kent, A. C. Kummel and R. Droopad. *J. Appl. Phys.* **110**, 013713 (2011).
4. T. Schneider, D. Aldrich, J. Cho and R. Nemanich. *MRS Proceedings*. **220**, 21 (1991).
5. S. W. Park, T. Kaufman-Osborn, H. Kim, S. Siddiqui, B Sahu, N. Yoshida, A Brandt and A. Kummel. *JVSTA* **33**, 041403 (2015).
6. B. Anthony, L. Breaux, T. Hsu, S. Banerjee and A. Tasch. *JVSTB: Microelectronics processing and phenomena.* **7**, 621-626 (1989).
7. P. Zalm. *Pure Appl. Chem.* **57**, 1253-1264 (1985).
8. *Handbook of silicon wafer cleaning technology*. K. Reinhardt and K. Werner editors. William Andrew, (2008).
9. M. Edmonds, W. Melitz, T. Kent, E. Chagarov and A. C. Kummel. *ECS Trans.,* **50**, 129-140 (2012).
10. S. Pearton. *Mater. Sci. Eng. : B.* **10**, 187-196 (1991).
11. C. D. Wagner. *Farad. Discuss.* **60**, 291-300 (1975).
12. G. Cossu, G. M. Ingo, G. Mattogno, G. Padeletti and G. M. Proietti. *Appl. Surf. Sci.* **56,** 81-88 (1992).
13. F. Aguirre-Tostado, M. Milojevic, C. L. Hinkle, E. M. Vogel, R. M. Wallace, S. McDonnell and S. Hughes. *Appl. Phys Lett.* **92**, 171906-171901 (2008).
14. M. Yamada, Y. Ide and K. Tone. *Jpn. J. Appl. Phys.* **31**, L1157 (1992).
15. P. Tomkiewicz, A. Winkler and J. Szuber. *Appl. Surf. Sci.* **252**, 7647-7658 (2006).
16. X. Zhang, E. Garfunkel, Y. Chabal, S. Christman and E. Chaban. *Appl. Phys. Lett.* **79**, 4051-4053 (2001).
17. S. Rivillon, Y. J. Chabal, F. Amy and A. Kahn. *Appl. Phys. Lett.* **87**, 253101 (2005).

18. Y. Chabal, G. Higashi, K. Raghavachari and V. Burrows. *JVSTA.* **7**, 2104-2109 (1989).
19. T. Kaufman-Osborn, K. Kiantaj, C.-P. Chang and A. C. Kummel. *Surf. Sci.* **630**, 254-259 (2014).
20. H. Nishino, N. Hayasaka and H. Okano. *J. Appl. Phys.* **74**, 1345-1348 (1993).
21. J. Kikuchi, M. Iga, H. Ogawa, S. Fujimura and H. Yano. *Jpn. J. Appl. Phys.* **33**, 2207 (1994).
22. P. Van Cleemput, G. Papasouliotis, M. Logan, B. Schravendijk and W. King. U.S. Patent No. 6,395,150. (2002).
23. T. Yew and R. Reif. *J. Appl. Phys.* **68**, 4681-4693 (1990).
24. K. S. Kim, W. E. Baitinger, J. W. Amy and N. Winograd. *J. Electron Spectros. Relat. Phenom.* **5.1**, 351-367 (1974).
25. D. Wagman, W. Evans, V. Parker, R. Schumm, I. Halow, S. Bailey, K. Churney and R. Luttall. *J. Phys. Chem. Ref. Data.* **11**, Supplement No. 2 (1982).
26. H. Ogawa, M. Y. Tomoharu Arai, T. Ichiki and Y. Horiike. *Jpn. J. of Appl. Phys.* **41**, 5349 (2002).
27. C. Kao, R. Arghavani and X. Lu. U.S. Patent No. EP1944796A2. (2008).